Published in final edited form as:

Heart Rhythm. 2017 May ; 14(5): 727–736. doi:10.1016/j.hrthm.2017.01.027.

Anti-arrhythmic effects of interleukin-1 inhibition following myocardial infarction

Nicole M. De Jesus, Ph.D.[1], **Lianguo Wang, M.D.**[2], **Johnny Lai, B.S.**[1], **Robert R. Rigor, Ph.D.**[2], **Samantha D. Francis Stuart, M.S.**[2], **Donald M. Bers, Ph.D.**[2], **Merry L. Lindsey, Ph.D.**[3], and **Crystal M. Ripplinger, Ph.D., FHRS**[2,*]

[1]Department of Biomedical Engineering, School of Engineering, University of California, Davis

[2]Department of Pharmacology, School of Medicine, University of California, Davis

[3]Mississippi Center for Heart Research, Department of Physiology and Biophysics, University of Mississippi Medical Center, Jackson, MS

Abstract

Background—Interleukin-1 beta (IL-1β) is a key regulator of the inflammatory response following myocardial infarction (MI), by modulating immune cell recruitment, cytokine production, and extracellular matrix turnover. Elevated levels of IL-1β are associated with adverse remodeling, and inhibition of IL-1 signaling following MI results in improved contractile function.

Objective—The goal of this study was to determine if IL-1 signaling also contributes to post-MI arrhythmogenesis.

Methods—MI was created in two murine models of elevated inflammation: atherosclerotic on Western diet or wild-type with a sub-septic dose of lipopolysaccharide. The role of IL-1β was assessed with the IL-1 receptor antagonist, anakinra (10mg/kg/day, starting 24h post-MI).

Results—*In vivo* and *ex vivo* molecular imaging showed reduced myocardial inflammation following a 4-day course of anakinra treatment, despite no change in infarct size. At day 5 post-MI, high-speed optical mapping of transmembrane potential (V_m) and intracellular Ca^{2+} in isolated hearts revealed that IL-1β inhibition improved conduction velocity, reduced action potential duration dispersion, improved intracellular Ca^{2+} handling, decreased V_m and Ca^{2+} alternans magnitude, and reduced spontaneous and inducible ventricular arrhythmias. These functional improvements were linked to increased expression of connexin43 and sarcoplasmic reticulum Ca^{2+}-ATPase (SERCA).

[*]**Corresponding author:** Crystal M. Ripplinger, Ph.D., FHRS, Department of Pharmacology, University of California Davis, 2219A Tupper Hall, One Shields Ave, Davis, CA 95616, Tel: 530-752-1569, cripplinger@ucdavis.edu.

Conflicts of Interest: None.

Disclosures

None.

Conclusions—This study revealed a novel mechanism for IL-1β in contributing to defective excitation-contraction coupling and arrhythmogenesis in the post-MI heart. Our results suggest that inhibition of IL-1 signaling post-MI may represent a novel anti-arrhythmic therapy.

Keywords

anti-arrhythmic agents; action potentials; calcium; interleukins; myocardial infarction

Introduction

Sudden cardiac death due to ventricular arrhythmias accounts for more than half of all cardiac-related deaths in the United States, and prior myocardial infarction (MI) increases the risk of sudden death ~6-fold.[1] Most MIs are due to coronary artery disease and rupture of an atherosclerotic plaque. Atherosclerosis is a chronic inflammatory disease[2] and studies in mouse models have revealed that underlying atherosclerosis significantly impacts remodeling and arrhythmia risk by altering the post-MI inflammatory response.[3–5] However, most pre-clinical studies of post-MI remodeling and arrhythmogenesis are performed in otherwise healthy animals, which do not reflect the underlying clinical pathophysiology and systemic inflammation occurring in patients with MI.

We recently showed that interleukin-1 beta (IL-1β) is upregulated ~3-fold in post-MI atherosclerotic versus post-MI wild-type mice.[5] Clinical evidence suggests that elevated levels of IL-1β at early post-MI time points are associated with impaired function, reduced left ventricular (LV) ejection fraction, and increased hypertrophy after 1 year.[6] Inhibition of IL-1 signaling following MI in pre-clinical and clinical studies has resulted in improved LV function and lower incidence of new-onset heart failure.[7–11] Despite these promising findings, the impact of IL-1β on excitation-contraction coupling and arrhythmogenesis post-MI has not been assessed. This is important because *in vitro* evidence suggests that IL-1β can impair cardiomyocyte Ca^{2+} homeostasis and disrupt gap junction coupling, both important contributors to arrhythmogenesis.

For example, treatment with IL-1β significantly reduces cardiomyocyte contractility,[12] reduces the amplitude and speed of Ca^{2+} transients,[13] and promotes sarcoplasmic reticulum (SR) Ca^{2+} leak and spontaneous arrhythmic activity when combined with other inflammatory cytokines.[14] Accompanying these changes are reductions in sacroplasmic reticulum Ca^{2+} ATPase (SERCA) at both the gene and protein level.[13] IL-1β has also been implicated in cell-cell uncoupling and slow conduction following MI via degradation of the ventricular gap junction protein, connexin43 (Cx43).[15,16] We therefore hypothesized that elevated IL-1β may be a key contributor to defective excitation-contraction coupling, slow conduction, and ventricular arrhythmia following MI.

To address this hypothesis, IL-1 signaling was inhibited in mouse models of MI using anakinra, an IL-1 receptor antagonist clinically used for the treatment of rheumatoid arthritis.[17] To reflect the large patient population with underlying coronary artery disease, MI was created in mice with either atherosclerosis or lipopolysaccharide (LPS)-induced inflammation, which we previously showed reproduces the atherosclerotic phenotype without confounding effects of hypercholesterolemia.[5]

Methods

An expanded methods section is available in the online supplement.

MI surgery

All procedures involving animals were approved by the Animal Care and Use Committee of the University of California Davis and adhered to the Guide for the Care and Use of Laboratory Animals published by the National Institutes of Health. Mice (n=36) were obtained from Jackson Laboratories and underwent MI (ischemia/reperfusion) surgery with 45 min of ischemia followed by reperfusion.[5] We have previously shown that this protocol produces a relatively small infarct, yet a robust arrhythmogenic substrate.[18]

Protocols are shown in Figure 1A. Starting 24h post-MI, all wild-type mice (n=16, C57BL/6 male, 12–14 weeks of age) were given daily injections of LPS (10μ g/day, I.P.) to reproduce the inflammatory response observed in atherosclerotic mice.[5] This low dose of LPS is ~25× lower than the septic dosage.[19] Apolipoprotein E deficient male mice on a C57BL/6 background ($ApoE^{-/-}$, n=20) were studied as a model of atherosclerosis. $ApoE^{-/-}$ mice were 24–26 weeks of age at the time of study following 10–12 weeks on Western diet (Harlan TD. 88137). A subset of $ApoE^{-/-}$ (n=8) and LPS-injected wild-type mice (n=7) were given daily injections of anakinra (ANA, 10mg/kg/day, I.P., starting 24h post-MI) and the remainder of the mice received sterile saline (0.9% NaCl) as control.

Optical imaging of inflammation

To assess inflammatory activity, mice were injected with ProSense750 FAST (0.16mol/kg, I.V., PerkinElmer) 24h post-MI (Day 1) and again on Day 4. *In vivo* optical imaging of ProSense750 was performed on post-MI days 2 and 5. *Ex vivo* optical imaging of excised hearts was also performed on day 5.[5]

Optical mapping of transmembrane potential (V_m) and intracellular Ca^2

On day 5 post-MI, hearts were excised and cannulated for Langendorff perfusion.[5] Blebbistatin (10–20μM) was added to the perfusate to reduce motion artifacts during optical recordings. Hearts were stained with voltage- and Ca^{2+}-sensitive dyes (RH237 and Rhod-2AM, respectively) for simultaneous optical mapping as previously described.[20] LV epicardial pacing was performed at a basic cycle length (BCL) of 150ms. Arrhythmia propensity was determined by an S1–S2 pacing protocol.[5] Alternans were induced with continuous pacing, decreasing in 10ms increments until loss of capture.

Optical mapping data analysis

Data were analyzed as previously described.[5] Action potential duration (APD) and AP rise time (Trise) were calculated from the infarct (area 9×5 pixels) located 4–6 pixels from the LAD suture (white boxes in Figure 3). Ventricular tachycardia (VT) was defined as lasting >3 beats. A score for severity of spontaneous arrhythmias was determined from the ECG as follows: 1=single premature ventricular complexes (PVCs), 2=bigeminy or salvos of PVCs, 3=VT (lasting >3 beats). Spectral methods were used to determine the presence of APD and Ca^{2+} alternans.[21]

Immunohistochemistry and protein analysis

Following imaging, half the hearts were randomly assigned to immunohistochemistry and histology experiments (n=3/group) and the other half to protein analysis (n=3/group). Proteins of interest included Cx43 and CD68 (for immunohistochemistry) and Cx43, IL-1β, SERCA, $Na_v1.5$, and α-actinin (loading control) for western blotting.

Infarct Size

Six short-axis cryosectioned slices at 0.5mm intervals were stained with hematoxylin and eosin for analysis of infarct size (Supplemental Figure 1).

Statistics

All variables are mean±SD. For most data sets, a one- or two-way ANOVA was performed with Tukey's multiple comparison post-testing. A Fisher's exact test was used to determine significance of arrhythmia inducibility. $P<0.05$ was considered statistically significant.

Results

Survival and infarct size

Three of 8 (37.5%) +LPS and 5 of 11 (45%) ApoE untreated mice died following MI compared to 1 of 7 (14%) +LPS+ANA and 1 of 8 (12.5%) ApoE+ANA mice (Figure 1B). All deaths occurred >24 hours post-surgery, indicating that surgical complications were unlikely and upon necropsy, no hearts displayed evidence of rupture. ANA treatment did not significantly impact infarct size at day 5 post-MI (Figure 1C).

IL-1 inhibition reduces myocardial inflammation

To assess myocardial inflammation, epifluorescent imaging of ProSense750 FAST was performed. We previously showed that ProSense fluorescence colocalizes with inflammatory cells in the post-MI heart.[5] Figure 2A and 2C show representative *in vivo* images of ProSense750 fluorescence over the time course of ANA treatment. At day 2, there are no significant differences in fluorescence intensity between groups. However, by day 5 there is a significant reduction in ProSense750 fluorescence in ANA-treated compared to untreated groups (Figure 2B–2C), indicating a reduction in inflammatory cell infiltration and activity. *Ex vivo* imaging of isolated hearts also showed a significant reduction in myocardial inflammation in the infarct region of interest (white box, Figure 2D) in +LPS+ANA and ApoE+ANA hearts (Figure 2D–2F).

IL-1 inhibition improves conduction velocity (CV), AP rise time, and APD dispersion

At day 5 post-MI, simultaneous optical mapping of V_m and intracellular Ca^{2+} was performed to assess electrophysiological remodeling, Ca^{2+} handling, and arrhythmia susceptibility. CV was significantly slower in the infarct versus non-infarct region of untreated hearts and this difference was mitigated with ANA (Figure 3B). ANA treatment also significantly improved CV in the infarct region of treated versus untreated hearts. ANA-treated ApoE hearts had shorter AP rise time (TRise) compared to untreated hearts and there was a trend for shorter TRise in treated +LPS hearts (Figure 3C–3D). Mean APD_{80} was not

significantly affected by ANA (Figure 3E–3F); however, treated ApoE hearts had decreased APD dispersion (Figure 3I). When all groups were pooled together, there was a significant positive correlation between inflammatory activity (as assessed by ProSense fluorescence) and TRise and a significant negative correlation between inflammation and CV (Figure 3G–3H).

IL-1 inhibition prevents spontaneous and inducible arrhythmias

A single premature pacing stimulus (S1–S2, Figure 4A) induced non-sustained VT in 4 of 6 (67%) +LPS and 3 of 6 (50%) ApoE hearts. ANA treatment prevented pacing-induced arrhythmia in all +LPS+ANA hearts (0/6) and reduced the occurrence in ApoE+ANA hearts (1/6, 17%, Figure 4B). Pacing-induced arrhythmias were reentrant in nature, and often, rotation near or around the infarct was visible. An example of reentrant arrhythmia induced by an S2 stimulus is shown in Supplemental Figure 2.

Spontaneous arrhythmic activity was also assessed and scored (Figure 4C). The arrhythmia score was higher in untreated compared to ANA-treated hearts (Figure 4D). Furthermore, no ANA-treated heart exhibited non-sustained VT (NS-VT >3 beats), which was present in untreated groups. Of those spontaneous PVCs captured with optical mapping, the activation maps were distinct from sinus rhythm with marked slowing of activation (Figure 4E).

Focal activity may arise due to diastolic Ca^{2+} elevation.[22] To assess propensity to diastolic Ca^{2+} elevation, burst pacing (duration 30sec) was performed in ApoE and ApoE+ANA hearts. Diastolic Ca^{2+} elevation, as seen in Figure 4F, was more frequent in untreated ApoE hearts (4/5) compared to ApoE+ANA (1/4). The diastolic Ca^{2+} elevation was most severe in the peri-infarct region (on average <1.5mm from the ligation site). Diastolic Ca^{2+} elevation was never observed in remote regions in any group.

IL-1 inhibition decreases APD and Ca^{2+} alternans

To assess alternans propensity, hearts were paced at increasing frequency until loss of capture. Figure 5A shows representative maps of the spectral magnitude of Ca^{2+} alternans in a +LPS and +LPS+ANA heart showing severe Ca^{2+} alternans at faster BCL (80ms) in the untreated heart. Example V_m and Ca^{2+} optical traces from these hearts are shown in Figure 5B. A summary of the average Ca^{2+} alternans spectral magnitude is shown in Figure 5C. The pacing threshold at which significant APD alternans first emerged was significantly slower in untreated +LPS versus +LPS+ANA hearts, but was unchanged in ApoE versus ApoE+ANA hearts (Figure 5D). The pacing threshold at which significant Ca^{2+} alternans first emerged was reduced by ANA treatment in both groups (Figure 5D), suggesting a strong effect of IL-1 inhibition on intracellular Ca^{2+} handling. Reductions in SERCA function may be associated with Ca^{2+} alternans;[23] therefore, we assessed the time constant of decay (*tau*) of the intracellular Ca^{2+} transient as a measure of SERCA activity. ANA significantly accelerated *tau* in the ApoE versus ApoE+ANA group (Figure 5E) and there was a trend for decreased tau in the +LPS+ANA group.

IL-1 inhibition alters Cx43 and SERCA protein expression

In vitro assays demonstrate that IL-1β down-regulates Cx43 in both brain and heart.[15,16,24] To assess expression of Cx43, infarct sections were co-labeled for Cx43 and the macrophage marker CD68. ANA treatment reduced the number of infiltrating macrophages in the infarct (Figure 6A vs. 6B). Furthermore, untreated hearts displayed marked Cx43 loss in areas of macrophage infiltration (Figure 6A, 6C), whereas ANA-treated hearts had little to no Cx43 down-regulation (Figure 6D), suggesting that inhibition of IL-1 signaling protects Cx43 in the infarct area. Western blotting revealed a significant increase in total Cx43 protein expression in +LPS+ANA hearts and a trend for increased expression in ApoE+ANA hearts (Figure 6E, 6G). Voltage-gated Na^+ channels also play an important role in CV and excitability; therefore expression of $Na_v1.5$ was assessed and showed no significant differences with ANA treatment (Supplemental Figure 3).

Given the known role of IL-1β in SERCA downregulation[13] and our finding of accelerated Ca^{2+} transient decay (Figure 5), total SERCA protein levels were assessed. ANA treatment significantly increased SERCA expression in the ApoE group, but had no effect in the LPS hearts (Figure 6F, 6H).

ANA treatment does not alter IL-1β expression

Anakinra is an IL-1 receptor antagonist; therefore, ANA treatment is not expected to decrease levels of IL-1β *per se*. Indeed, there were no significant differences in IL-1β expression in either group (Figure 6F, 6I). This result is consistent with previous studies with anakinra in the post-MI setting.[11]

Discussion

IL-1β is a key regulator of the post-MI inflammatory response, and recent clinical and experimental studies have demonstrated improvements in LV function with IL-1 inhibition following MI.[7–11] Here we show, for the first time, that IL-1 signaling also plays an important role in post-MI electrophysiological remodeling and arrhythmogenesis. A four-day course of treatment with the FDA-approved IL-1 receptor antagonist, anakinra, reduced spontaneous and inducible arrhythmias despite no change in infarct size. Our findings demonstrate that IL-1β inhibition improved cell-cell coupling and normalized Ca^{2+} homeostasis, which collectively reduced the propensity to triggered and reentrant arrhythmias.

IL-1 signaling

Both IL-1α and IL-1β bind to the interleukin-1 receptor type 1 (IL-1R1). The same cells that produce IL-1α and IL-1β also produce a naturally occurring IL-1 receptor antagonist (IL-1Ra), which competitively binds to IL-1R1 and inhibits signaling. Anakinra is a recombinant human IL-1Ra that is routinely used for the treatment of rheumatoid arthritis.[17] Although anakinra inhibits both IL-1α and IL-1β signaling, these cytokines have nearly identical biological activity and IL-1β is the main circulating form of IL-1.[25]

IL-1 signaling may recruit additional inflammatory cells to the MI and induce subsequent IL-1β production. Therefore, by inhibiting the IL-1 signaling cascade, anakinra *may* reduce levels of IL-1β production. To test for this, we quantified mature IL-1β expression from the infarct area and found no significant differences in IL-1β expression (although there was a trend for decreased IL-1β in ANA-treated ApoE hearts, Figure 6F, 6I). These findings are consistent with previous studies of anakinra in the post-MI heart where IL-1β expression was also unchanged.[11]

Several clinical and pre-clinical studies have demonstrated improvements in structural remodeling and LV function with IL-1 inhibition following MI.[8,10,11] Investigations into underlying mechanisms have reported reduced immune cell recruitment, accelerated resolution of inflammation, reduced fibrosis, and attenuated cardiomyocyte apoptosis as contributors to improved post-MI function.[7,10,11] Despite these favorable findings, very little is known about the direct role of IL-1 signaling on excitation-contraction coupling and ventricular arrhythmias following MI.

IL-1β and intracellular Ca^{2+} homeostasis

IL-1β is a negative inotrope, and acute treatment with IL-1β results in decreased amplitude and speed of the intracellular Ca^{2+} transient, decreased SR Ca^{2+} content, and increased spontaneous SR Ca^{2+} release.[12,14] Chronic exposure of cardiomyocytes to IL-1β leads to reduced expression of SERCA and its regulatory protein, phospholamban.[13,26] Importantly, these changes in intracellular Ca^{2+} handling are not only expected to decrease cardiomyocyte contractility, but may also contribute to Ca^{2+}-mediated arrhythmia.[22]

Our findings in the post-MI mouse heart are consistent with *in vitro* studies and suggest that IL-1β may be a significant contributor to altered Ca^{2+} homeostasis following MI. Inhibition of IL-1 signaling resulted in fewer PVCs and focal arrhythmias, and fewer instances of pathological diastolic Ca^{2+} elevation (Figure 4F). Moreover, anakinra significantly attenuated beat-to-beat alternation of the Ca^{2+} transient and APD (Figure 5), the underlying causes of arrhythmogenic T-wave alternans. Several experimental studies have demonstrated that beat-to-beat alternation in the amount of Ca^{2+} released from the SR may underlie alternans.[21,27] Therefore, a reduction in the magnitude of Ca^{2+} alternans, or an increase in the heart rate at which Ca^{2+} alternans first appears (both observed in the present study with ANA, Figure 5), are indicators of improved Ca^{2+} homeostasis and decreased arrhythmia risk.

Decreased SERCA activity is also associated with increased Ca^{2+} alternans magnitude[23] and ANA treatment resulted in acceleration of the time constant of Ca^{2+} decay (*tau*) in ApoE hearts. Consistent with this, total SERCA expression was significantly increased in the ApoE+ANA group compared to untreated ApoEs, whereas SERCA expression was unaffected in the +LPS hearts (Figure 6). These results may suggest differential regulation of SERCA expression by IL-1 in ApoE versus +LPS hearts.

IL-1β and Cx43

First observed in astrocytes and later in cardiomyocytes, *in vitro* administration of IL-1β reduces Cx43 at both the gene and protein level.[15,16,24] Although many cell types can

release IL-1β, including endothelial cells, cardiomyocytes, and myofibroblasts, once inflammatory cells are recruited to the infarct, they are likely a major source of IL-1β.[25] Indeed, we previously reported significant degradation and lateralization of Cx43 in areas of macrophage infiltration, suggesting that macrophage-secreted factors may be influencing Cx43 expression.[5] In the present study, we found that IL-1 inhibition preserved Cx43 expression and distribution, even in regions with significant macrophage infiltration (Figure 6C vs. 6D), suggesting that macrophage infiltration *per se* does not influence Cx43 and that blocking IL-1 signaling in cardiomyocytes is likely responsible for preserved Cx43. The mechanism of IL-1β-mediated Cx43 degradation remains unknown, but studies in astrocytes suggest that IL-1β results in replacement of Cx43 gap junction proteins with the tight junction protein, claudin-1.[24] Whether a similar mechanism of cell junction replacement occurs in cardiomyocytes is an area for future study.

Total Cx43 protein expression was significantly increased in +LPS+ANA infarcts and there was a trend for increased Cx43 expression in ApoE+ANA infarcts (Figure 6). We also observed modest, yet significant improvements in CV in both ANA-treated groups (Figure 3). Since total Na^+ channel expression was unaltered with ANA treatment (Supplemental Figure 3), these results suggest that increased Cx43 expression may be a mediator of improved conduction in this case.

Clinical Implications

Currently, there is significant clinical interest in the role of IL-1 signaling in ischemic heart disease. In particular, the Canakinumab Anti-inflammatory Thrombosis Outcomes Study (CANTOS) will test whether treatment with canakinumab, a human monoclonal IL-1β antibody, inhibits atherothrombosis to reduce rates of recurrent MI and stroke among patients with coronary artery disease.[28] Smaller clinical studies have investigated the use of anakinra to limit adverse left ventricular remodeling and new onset heart failure following MI.[8,9] However, no clinical nor pre-clinical study to date has assessed the impact of IL-1 inhibition on post-MI electrophysiological remodeling and arrhythmias, important clinical outcomes given that sudden cardiac death due to ventricular arrhythmias may account for approximately one-third of cardiovascular-related post-MI mortality.[29]

Study Limitations

The goal of our study was to assess the efficacy of IL-1 inhibition in a clinically relevant animal model of coronary heart disease. Therefore, MI was created in $ApoE^{-/-}$ mice on atherogenic diet and wild-type mice treated with LPS, which we and others have shown reproduces the ApoE phenotype.[3,5] Untreated wild-type mice with MI and sham-operated mice were not evaluated in the present study, but a previous report by our group details direct comparisons between ApoE, +LPS, untreated wild-type, and sham hearts.[5] Risk for post-MI arrhythmias decreases sharply over time; we therefore chose an early, 5 day time point for study. The long-term effects of anakinra on post-MI arrhythmias remain to be evaluated and it will be increasingly important to assess markers of structural remodeling and fibrosis as the scar matures. Although infarct size was similar between groups, there may be variation in the location of the infarct relative to the mapping field of view. This

variation may impact measurements of APD dispersion, which were calculated across the entire epicardial surface. Reperfused MIs are typically more patchy and diffuse, with heterogeneous distribution of myocytes, inflammatory cells, and fibrotic scar. At 5 days post-MI, this model does not produce a clear endo- or epicardial border zone; therefore, the infarct region was objectively defined based on the suture location and it was histologically verified that this region contained infarct and peri-infarct tissue. Finally, our results point toward an increase in total Cx43 expression as a mediator of improved CV, but we did not assess lateralization or phosphorylation status of Cx43, which are also important contributors to conduction.

Supplementary Material

Refer to Web version on PubMed Central for supplementary material.

Acknowledgments

Sources of funding:

This study was funded by the NIH (R01 HL111600 to C.M.R., R01 HL030077 to D.M.B., R01 HL075360 to M.L.L., and T32 GM099608 to N.M.D., S.D.S.F., and D.M.B.) and the American Heart Association (12SDG9010015 to C.M.R.).

References

1. Mozaffarian D, Benjamin EJ, Go AS, et al. Heart Disease and Stroke Statistics-2016 Update: A Report From the American Heart Association. Circulation. 2016; 133:e38–e360. [PubMed: 26673558]
2. Libby P. Inflammation in atherosclerosis. Nature. 2002; 420:868–874. [PubMed: 12490960]
3. Panizzi P, Swirski FK, Figueiredo JL, Waterman P, Sosnovik DE, Aikawa E, Libby P, Pittet M, Weissleder R, Nahrendorf M. Impaired infarct healing in atherosclerotic mice with Ly-6C(hi) monocytosis. J Am Coll Cardiol. 2010; 55:1629–1638. [PubMed: 20378083]
4. Nahrendorf M, Swirski FK, Aikawa E, Stangenberg L, Wurdinger T, Figueiredo JL, Libby P, Weissleder R, Pittet MJ. The healing myocardium sequentially mobilizes two monocyte subsets with divergent and complementary functions. J Exp Med. 2007; 204:3037–3047. [PubMed: 18025128]
5. De Jesus NM, Wang L, Herren AW, Wang J, Shenasa F, Bers DM, Lindsey ML, Ripplinger CM. Atherosclerosis exacerbates arrhythmia following myocardial infarction: Role of myocardial inflammation. Heart Rhythm. 2015; 12:169–178. [PubMed: 25304682]
6. Ørn S, Ueland T, Manhenke C, Sandanger Ø, Godang K, Yndestad A, Mollnes TE, Dickstein K, Aukrust P. Increased interleukin-1β levels are associated with left ventricular hypertrophy and remodelling following acute ST segment elevation myocardial infarction treated by primary percutaneous coronary intervention. J Intern Med. 2012; 272:267–276. [PubMed: 22243053]
7. Abbate A, Van Tassell BW, Seropian IM, Toldo S, Robati R, Varma A, Salloum FN, Smithson L, Dinarello CA. Interleukin-1beta modulation using a genetically engineered antibody prevents adverse cardiac remodelling following acute myocardial infarction in the mouse. Eur J Heart Fail. 2010; 12:319–322. [PubMed: 20335350]
8. Abbate A, Van Tassell BW, Biondi-Zoccai G, et al. Effects of interleukin-1 blockade with anakinra on adverse cardiac remodeling and heart failure after acute myocardial infarction. Am J Cardiol. 2013; 111:1394–1400. [PubMed: 23453459]
9. Abbate A, Kontos MC, Grizzard JD, et al. Interleukin-1 blockade with anakinra to prevent adverse cardiac remodeling after acute myocardial infarction. Am J Cardiol. 2010; 105:1371.e1371–1377.e1371. [PubMed: 20451681]

10. Sager HB, Heidt T, Hulsmans M, et al. Targeting Interleukin-1β Reduces Leukocyte Production After Acute Myocardial Infarction. Circulation. 2015; 132:1880–1890. [PubMed: 26358260]
11. Abbate A, Salloum FN, Vecile E, et al. Anakinra, a recombinant human interleukin-1 receptor antagonist, inhibits apoptosis in experimental acute myocardial infarction. Circulation. 2008; 117:2670–2683. [PubMed: 18474815]
12. Kumar A, Thota V, Dee L, Olson J, Uretz E, Parrillo JE. Tumor necrosis factor alpha and interleukin-1beta are responsible for in vitro myocardial cell depression induced by human septic shock serum. J Exp Med. 1996; 183:949–958. [PubMed: 8642298]
13. Combes A, Frye CS, Lemster BH, Brooks SS, Watkins SC, Feldman AM, McTiernan CF. Chronic exposure to interleukin-1beta induces a delayed and reversible alteration in excitation-contraction coupling of cultured cardiomyocytes. Pflugers Arch. 2002; 445:246–256. [PubMed: 12457245]
14. Duncan DJ, Yang Z, Hopkins PM, Steele DS, Harrison SM. TNF-alpha and IL-1beta increase Ca2+ leak from the sarcoplasmic reticulum and susceptibility to arrhythmia in rat ventricular myocytes. Cell Calcium. 2010; 47:378–386. [PubMed: 20227109]
15. Baum JR, Long B, Cabo C, Duffy HS. Myofibroblasts cause heterogeneous Cx43 reduction and are unlikely to be coupled to myocytes in the healing canine infarct. Am J Physiol Heart Circ Physiol. 2012; 302:H790–H800. [PubMed: 22101526]
16. Baum JR, Dolmatova E, Tan A, Duffy HS. Omega-3 fatty acid inhibition of inflammatory cytokine-mediated Connexin43 regulation in the heart. Front Physiol. 2012; 3:272. [PubMed: 22934026]
17. Ikonomidis I, Lekakis JP, Nikolaou M, Paraskevaidis I, Andreadou I, Kaplanoglou T, Katsimbri P, Skarantavos G, Soucacos PN, Kremastinos DT. Inhibition of interleukin-1 by anakinra improves vascular and left ventricular function in patients with rheumatoid arthritis. Circulation. 2008; 117:2662–2669. [PubMed: 18474811]
18. Gardner RT, Wang L, Lang BT, Cregg JM, Dunbar CL, Woodward WR, Silver J, Ripplinger CM, Habecker BA. Targeting protein tyrosine phosphatase-σ after myocardial infarction restores cardiac sympathetic innervation and prevents arrhythmias. Nat Commun. 2015; 6:6235. [PubMed: 25639594]
19. Remick DG, Newcomb DE, Bolgos GL, Call DR. Comparison of the mortality and inflammatory response of two models of sepsis: lipopolysaccharide vs. cecal ligation and puncture. Shock. 2000; 13:110–116. [PubMed: 10670840]
20. Myles RC, Wang L, Kang C, Bers DM, Ripplinger CM. Local β-adrenergic stimulation overcomes source-sink mismatch to generate focal arrhythmia. Circ Res. 2012; 110:1454–1464. [PubMed: 22539768]
21. Wang L, Myles RC, De Jesus NM, Ohlendorf AKP, Bers DM, Ripplinger CM. Optical mapping of sarcoplasmic reticulum Ca2+ in the intact heart: ryanodine receptor refractoriness during alternans and fibrillation. Circ Res. 2014; 114:1410–1421. [PubMed: 24568740]
22. Bers DM. Cardiac excitation-contraction coupling. Nature. 2002; 415:198–205. [PubMed: 11805843]
23. Cutler MJ, Wan X, Plummer BN, Liu H, Deschênes I, Laurita KR, Hajjar RJ, Rosenbaum DS. Targeted sarcoplasmic reticulum Ca(2+) ATPase-2a gene delivery to restore electrical stability in the failing heart. Circulation. 2012; 126:2095–2104. [PubMed: 23019291]
24. Duffy HS, John GR, Lee SC, Brosnan CF, Spray DC. Reciprocal regulation of the junctional proteins claudin-1 and connexin43 by interleukin-1beta in primary human fetal astrocytes. J Neurosci. 2000; 20:RC114. [PubMed: 11090614]
25. Bujak M, Frangogiannis NG. The role of IL-1 in the pathogenesis of heart disease. Arch Immunol Ther Exp (Warsz). 2009; 57:165–176. [PubMed: 19479203]
26. McTiernan CF, Lemster BH, Frye C, Brooks S, Combes A, Feldman AM. Interleukin-1beta inhibits phospholamban gene expression in cultured cardiomyocytes. Circ Res. 1997; 81:493–503. [PubMed: 9314830]
27. Picht E, Desantiago J, Blatter LA, Bers DM. Cardiac alternans do not rely on diastolic sarcoplasmic reticulum calcium content fluctuations. Circ Res. 2006; 99:740–748. [PubMed: 16946134]

28. Ridker PM, Thuren T, Zalewski A, Libby P. Interleukin-1β inhibition and the prevention of recurrent cardiovascular events: rationale and design of the Canakinumab Anti-inflammatory Thrombosis Outcomes Study (CANTOS). Am Heart J. 2011; 162:597–605. [PubMed: 21982649]

29. Bougouin W, Marijon E, Puymirat E, et al. Incidence of sudden cardiac death after ventricular fibrillation complicating acute myocardial infarction: a 5-year cause-of-death analysis of the FAST-MI 2005 registry. Eur Heart J. 2014; 35:116–122. [PubMed: 24258072]

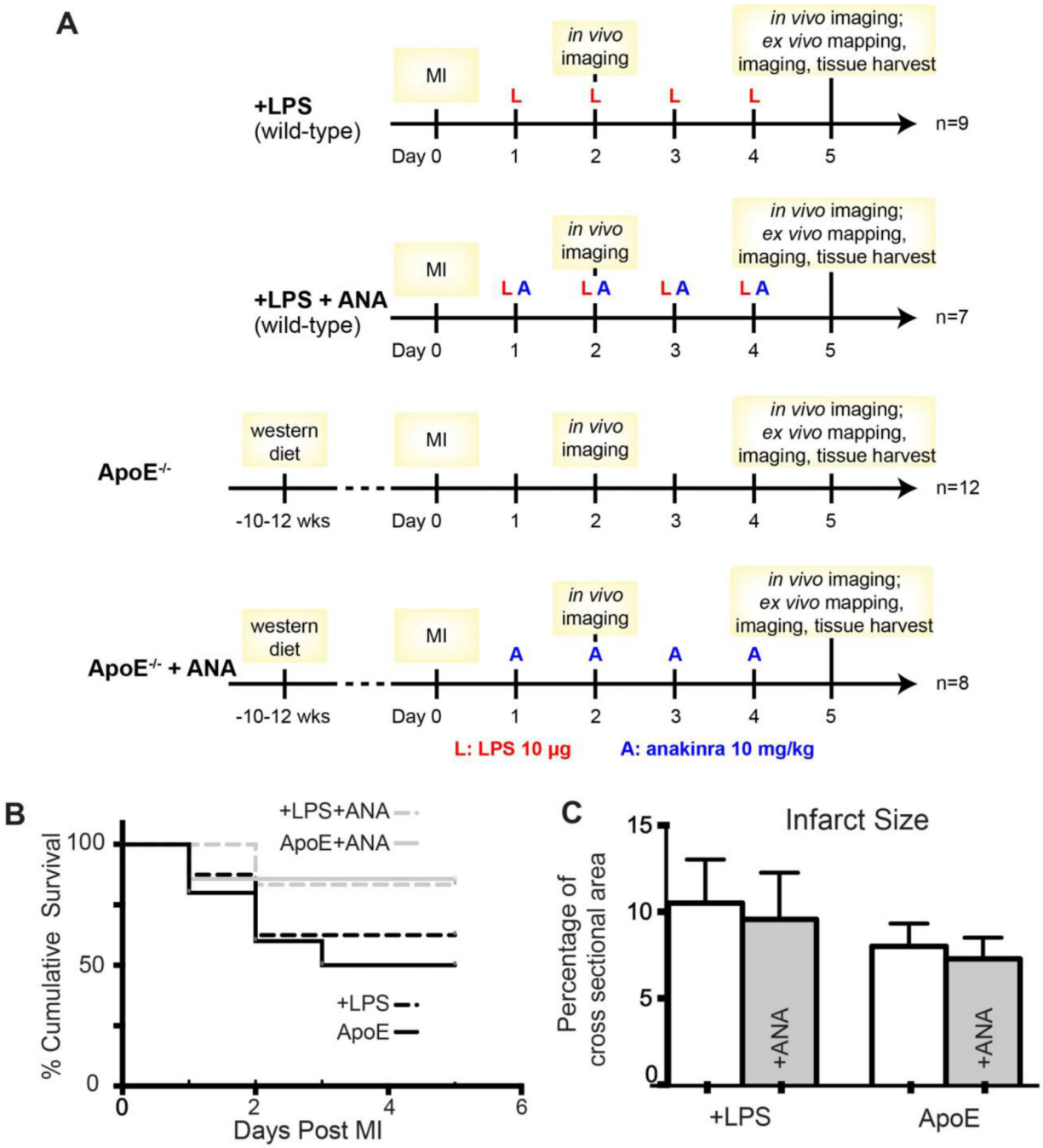

Figure 1.

A) Experimental design. **B)** Post-MI survival. **C)** Infarct size. ANA: anakinra.

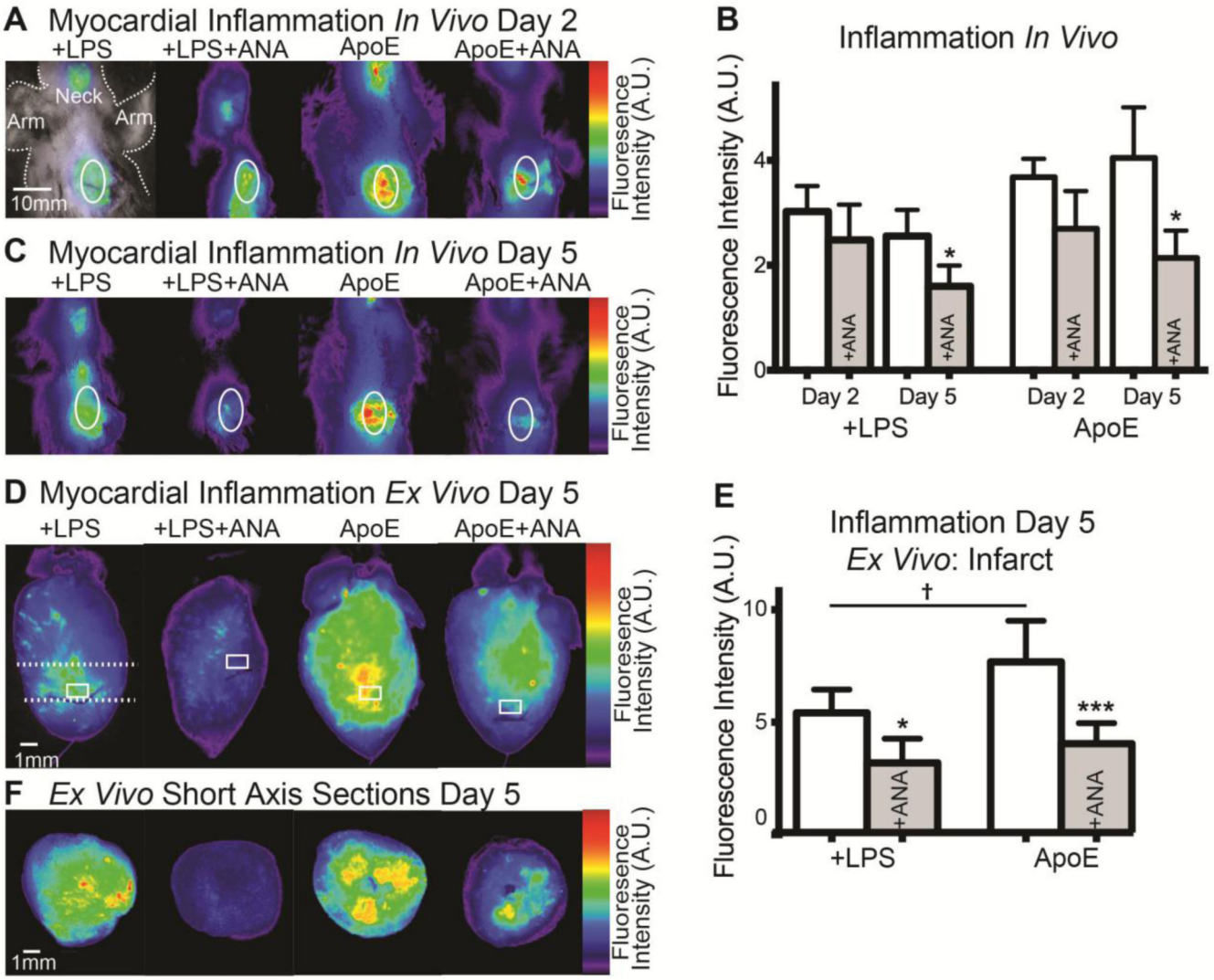

Figure 2.

A) *In vivo* imaging of ProSense750 at day 2 post-MI. White oval indicates heart. The neck also shows mild inflammation due to a surgical incision to ensure intubation. **B)** No significant differences in myocardial inflammation are observed at day 2, but significant reductions are observed by day 5 in both ANA-treated groups. **C)** *In vivo* imaging of ProSense750 at day 5 post-MI. **D)** *Ex vivo* imaging of ProSense750 from isolated hearts at day 5 post-MI. White box indicates infarct region of interest (ROI). **E)** Quantification of *ex vivo* infarct ROI fluorescence. **F)** *Ex vivo* imaging of ProSense750 in short-axis slices. Dashed white line in (D) indicates location of slice. *p<0.05, ***p<0.001 +LPS vs. +LPS +ANA or ApoE vs. ApoE+ANA. †p<0.05 +LPS vs. ApoE.

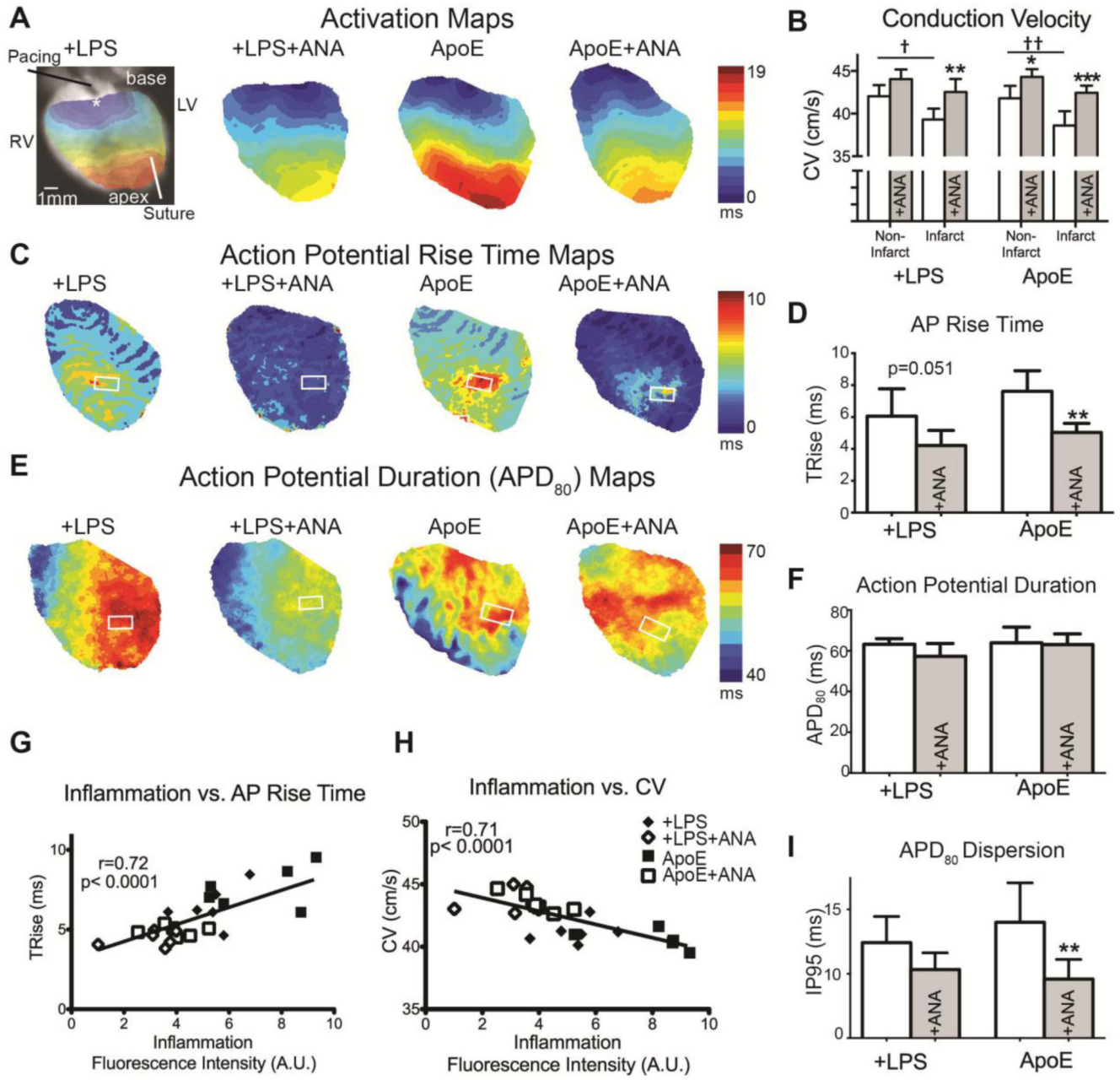

Figure 3.

A) Activation maps during LV pacing. **B)** CV was assessed in the non-infarct (area proximal to the suture) and infarct (area distal to the suture) regions. Untreated hearts had significantly slower CVs in the infarct vs. non-infarct regions. These differences were mitigated with ANA. Additionally, ANA treatment significantly improved CV in the infarct region of treated vs. untreated hearts. **C)** Maps of action potential rise time (TRise). **D)** TRise from the infarct region (white box in C). **E)** Maps of action potential duration at 80% repolarization (APD_{80}). **F)** No significant differences were observed in APD_{80} in the infarct region (white box in E). **G)** When all groups were pooled, a significant positive correlation was observed

between inflammation intensity (ProSense750 fluorescence) and TRise in the infarct ROI. **H)** A significant negative correlation was observed between inflammation intensity and mean CV. **I)** APD dispersion was calculated across the entire epicardial field of view as the inner 95^{th} percentile (IP95: range over which 95% of the data lie). †$p<0.05$, ††$p<0.01$ non-infarct vs. infarct; *$p<0.05$, **$p<0.01$, ***$p<0.001$ +LPS vs. +LSP+ANA or ApoE vs. ApoE +ANA.

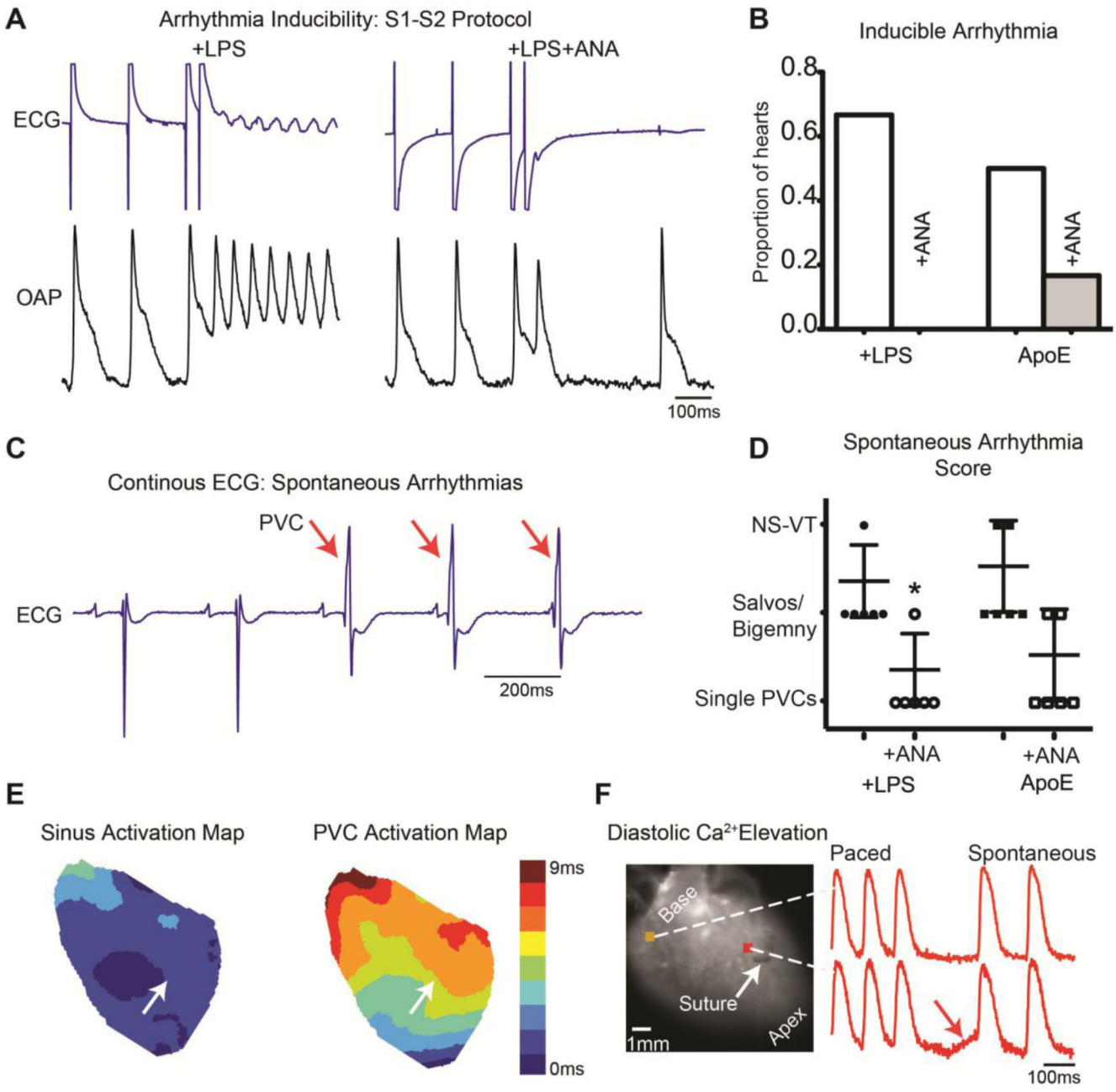

Figure 4.

A) Example S1–S2 pacing protocol in which a reentrant arrhythmia was induced in a +LPS but not +LPS+ANA heart. **B)** Proportion of hearts with inducible arrhythmias. **C)** Example ECG from an ApoE heart with 3 spontaneous PVCs indicated with red arrows. **D)** ANA treatment significantly reduced the severity of spontaneous arrhythmias in +LPS hearts. **E)** Activation map during sinus rhythm (left) and PVC (right) from a +LPS heart. White arrow indicates suture location. Note the slower total activation time and different pattern of activation during the PVC, with earliest activation emerging apical to the infarct. **F)** Example of diastolic Ca^{2+} elevation following rapid pacing. The final 3 paced beats are

shown followed by a diastolic interval in which spontaneous diastolic Ca^{2+} elevation is observed in the infarct region of an untreated ApoE heart. In this example, diastolic Ca^{2+} elevation is interrupted by a sinus beat. *p<0.05 +LPS vs. +LPS+ANA.

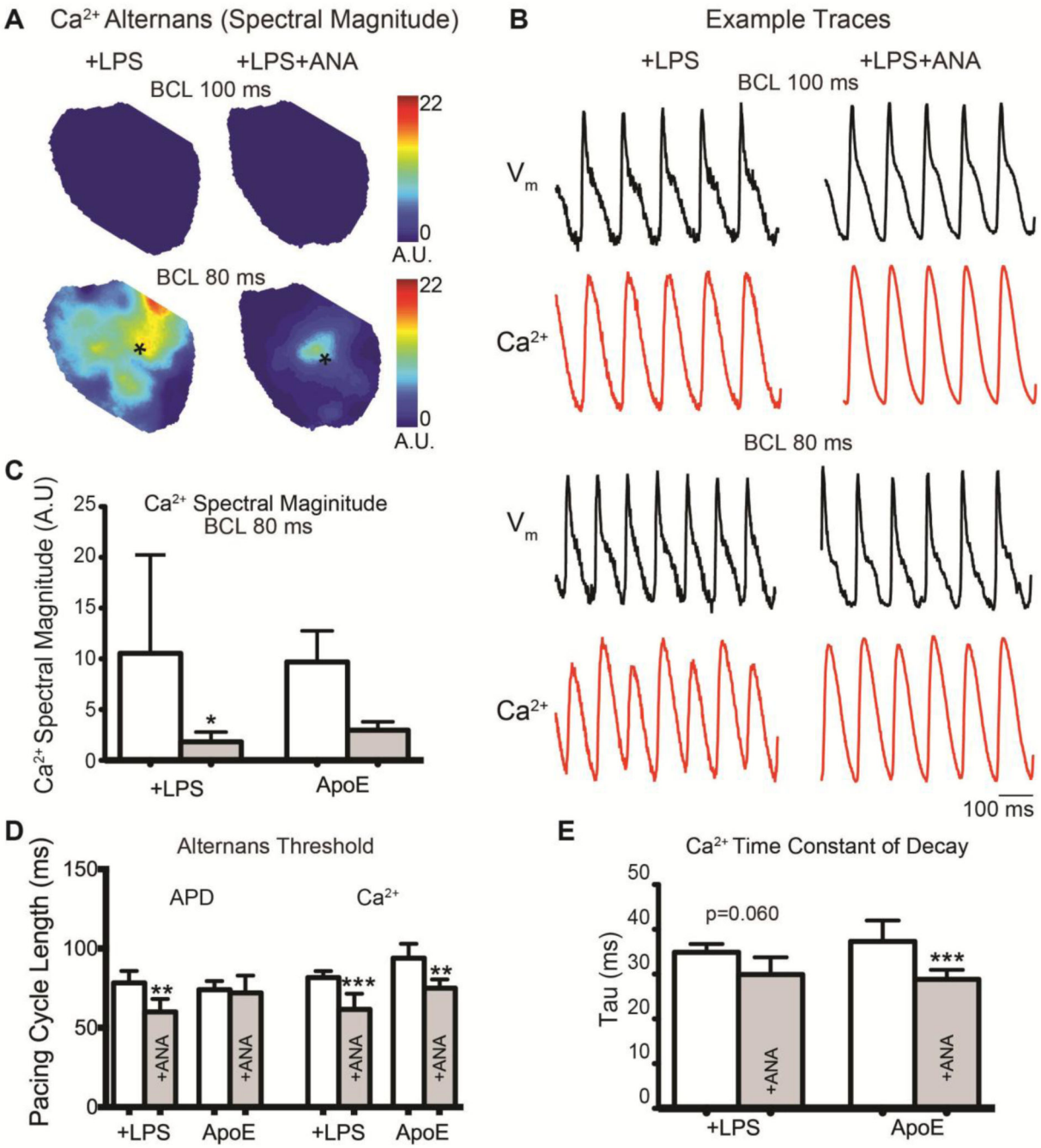

Figure 5.

A) Maps of Ca^{2+} alternans spectral magnitude at BCL=100ms (top) and BCL=80ms (bottom). **B)** Example optical V_m and intracellular Ca^{2+} traces from the hearts shown in (A) with the signal location indicated with an asterisk. **C)** The average Ca^{2+} alternans spectral magnitude was quantified at BCL=80ms. **D)** The pacing cycle length at which hearts first displayed significant APD or Ca^{2+} alternans (spectral magnitude ≥ 2). **E)** The time constant of decay (*tau*) of the intracellular Ca^{2+} transient. *p<0.05, **p<0.01, ***p<0.001 +LPS vs. +LPS+ANA or ApoE vs. ApoE+ANA.

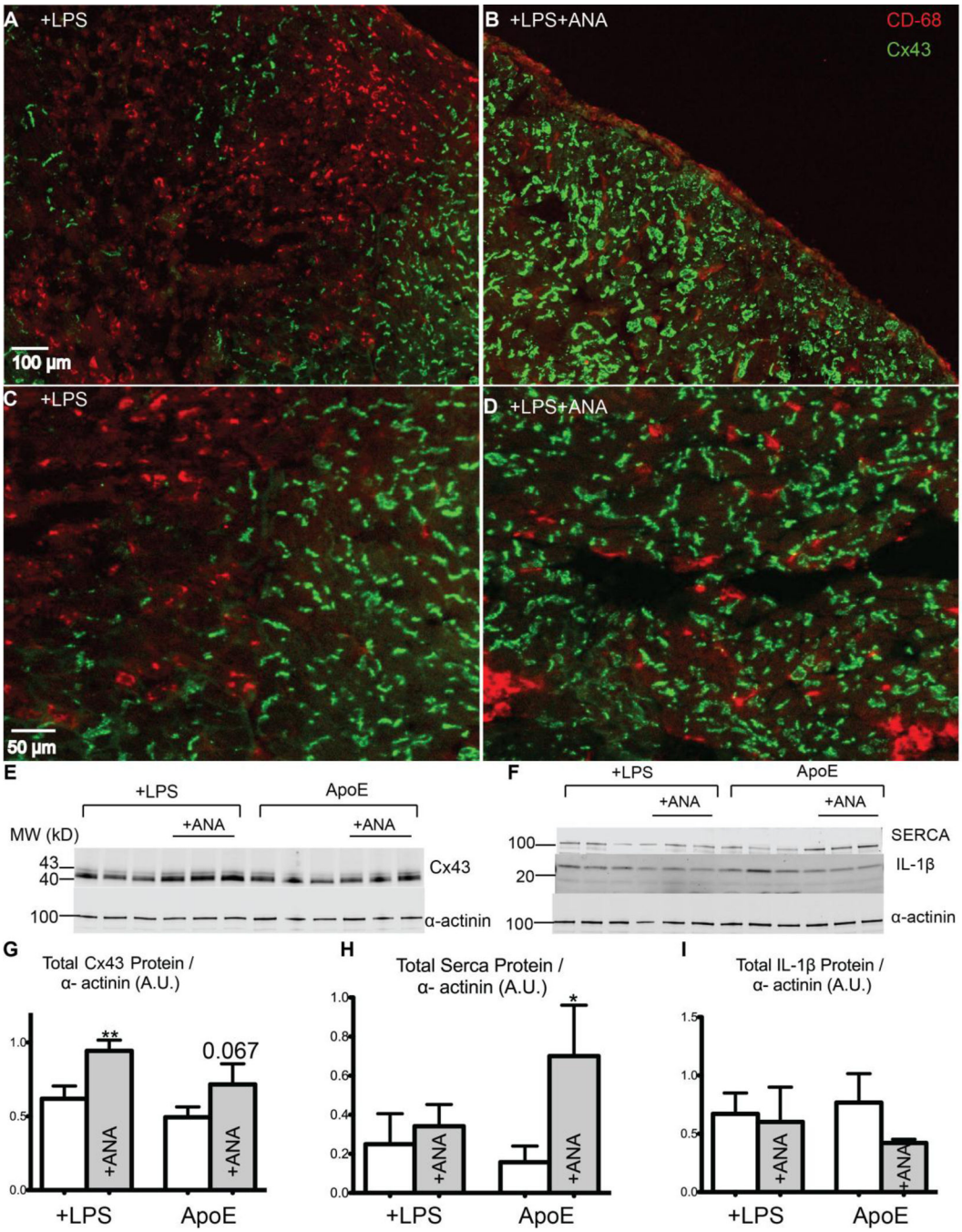

Figure 6.

A–B) Immunohistochemistry images of the infarct area of a +LPS (**A**) and a +LPS+ANA (**B**) heart with CD68 staining for macrophages (red) and Cx43 staining (green). Note the abundant CD68-positive staining in the infarct region of the +LPS heart. **C)** Magnified image showing a near-complete loss of Cx43 in CD68-positive areas of a +LPS heart. **D)** Robust Cx43 expression in a +LPS+ANA heart, even in areas of CD68-positive cells. **E)** Immunoblot of Cx43 and α-actinin (loading control). **F)** Immunoblot of SERCA, IL-1β, and α-actinin. **G)** Total Cx43 protein expression. **H)** Total SERCA protein expression. **I)** Total

IL-1β protein expression. *p<0.05, **p<0.01 +LPS vs. +LPS+ANA or ApoE vs. ApoE +ANA.